Salt–Induced Contraction of Polyelectrolyte Diblock Copolymer Micelles

2 AUTHORS, INCLUDING:

Johan R C van der Maarel

108 PUBLICATIONS **1,716** CITATIONS

Salt-Induced Contraction of Polyelectrolyte Diblock Copolymer Micelles

J. R. C. van der Maarel* and W. Groenewegen

Leiden Institute of Chemistry, Gorlaeus Laboratories, Leiden University, PO Box 9502, 2300 RA Leiden, The Netherlands

S. U. Egelhaaf

Department of Physics and Astronomy, JCMB, University of Edinburgh, Edinburgh EH9 3JZ, United Kingdom

A. Lapp

Laboratoire Léon Brillouin, CE de Saclay, 91191 Gif-sur-Yvette Cedex, France

To describe the effect of salt on the structural arrangement of the blocks in aqueous poly(styrene-*block*-acrylic acid) [PS(20)-*b*-PA(85)] solutions, the partial structure factors pertaining to PS−PS and PA−PA density correlations, as well as the composition structure factor were obtained with small-angle neutron scattering and contrast matching in the water. The copolymers self-assemble with an aggregation number ~100 into spherical micelles made of a PS-block core, surrounded by a coronal layer formed by the PA blocks. The addition of salt has no effect on the size of the core and the aggregation number. At full corona charge and minimal screening conditions, the PA chains are almost fully stretched in the radial direction away from the core. With increasing salt concentration, the micelle contracts and the corona chain statistics can be described with a two-region density-scaling model. In the inner coronal region the statistics is unaffected by the salt, whereas for larger radial distances the scaling is similar to neutral polymer stars. Both the micelle radii and the crossover distance between the two different density-scaling regimes comply with theory for osmotic star-branched polyelectrolytes in the salt-dominated regime. For low fractional corona charge, the density scaling is determined by charge annealing effects. Here, the addition of salt does not affect the density scaling, but the micelle nevertheless contracts and eventually precipitates at high ionic strength. Despite the high salt concentrations required to compete with the salinity in the coronal layer generated by the counterions coming from the polyelectrolyte blocks, the range in micelle dimension is similar to the one that can be covered by variation in pH.

Introduction

Polyelectrolyte diblock copolymers comprise two linearly attached moieties: a charged and a hydrophobic chain part. The hydrophobic attachment provides a mechanism for bringing the copolymers together, and mesoscopic structures of surprising complexity can be formed. These structures include spherical micelles, wormlike cylinders, lamellae, and (compound) vesicles with a size larger than the molecular dimension of the copolymer building blocks.[1,2] Fine regulation of the interactions through variation of the charge, ionic strength, and respective block sizes gives unprecedented control of the morphology, which cannot be realized with neutral, amphiphilic copolymers. Polyelectrolyte diblock copolymers have considerable potential in industrial applications; due to the increased need of water supported systems. Furthermore, the brushes made of the polyelectrolyte blocks are thought to be a model of the external envelope of some microorganisms and, hence, progress in this area might have important implications for other fields such as biophysics.[3,4]

In previous work, we have investigated simple salt-free micelles of the diblock copolymer poly(styrene-*block*-acrylic acid) [PS(20)-*b*-PA(85)] with small-angle neutron scattering (SANS) and block contrast variation in the water.[5] These copolymers self-assemble with an aggregation number ~100 into spherical micelles made of a densely packed, glassy, spherical PS-block core (with a radius 4.5 nm), surrounded by a coronal layer formed by the PA blocks. The extension of the PA chains and, hence, the micelle radius, were found to be highly sensitive to the degree of ionization of the weak polyacid block. The degree of ionization was controlled by pH, specifically the addition of base to solutions in the acid form. At full ionization, the PA chains are almost fully stretched with a density scaling proportional to the inverse second power of the radius away from the core. This behavior is strikingly different from the situation for neutral spherical polymer brushes, where the chains take a more compact, coiled conformation.[6,7] At a fractional corona charge less than 0.1, the results show the effects of charge annealing, i.e., migration of charges toward the outer coronal region due to the recombination and dissociation balance of the weak

---

* To whom correspondence should be addressed.

(1) Moffitt, M.; Khougaz, K.; Eisenberg, A. *Acc. Chem. Res.* **1996**, *29*, 95.

(2) Cameron, N. S.; Corbierre, M. K.; Eisenberg A. *Can. J. Chem.* **1999**, *77*, 1311.

(3) Tran, Y.; Auroy, P.; Lee, L.-T.; Stamm, M. *Phys. Rev. E* **1999**, *60*, 6984.

(4) Moat, A. G.; Foster, J. W. *Microbial Physiology*, 3rd ed.; Wiley-Liss: New York, 1995.

(5) Groenewegen, W.; Egelhaaf, S. U.; Lapp, A.; van der Maarel, J. R. C. *Macromolecules* **2000**, *33*, 3283.

(6) Daoud M.; Cotton, J.-P. *J. Phys.* (*Paris*) **1982**, *43*, 531.

(7) Förster, S.; Wenz, E.; Lindner, P. *Phys. Rev. Lett.* **1996**, *77*, 95.

polyacid. The dimension of the micelles and the corona chain statistics were interpreted with scaling approaches for star-branched polyelectrolytes.[8−10] Furthermore, with SANS and contrast variation in the (tetramethylammonium) counterion, we have shown that at a fractional charge 0.5 all counterions are trapped in the coronal layer with a radial distribution very close to the one for the segments of the corona-forming blocks.[11]

Our previous experiments were done without added salt, and, hence, the main contribution to the corona stretching force is given by the osmotic pressure exerted by the counterions trapped in the coronal layer (osmotic regime). In the presence of salt, the additional screening of Coulomb interaction results in a contraction of the micelle. Rather high salt concentrations are required, because charged brushes generate their own salinity with the counterions coming from the corona-forming polyelectrolyte blocks. Experiments on poly(*tert*-butylstyrene-*block*-sodium styrenesulfonate) (PtBS-*b*-NaPSS) copolymers have shown that the micelles indeed decrease in size with increasing salt concentration, but the salt dependence was found to be weaker than predicted by theory.[12,13] In the latter experiments, an evaluation of the salt-induced contraction of the chains in the corona is complicated, due to a concurrent decrease in aggregation number at high salt (which is facilitated by the low glass transition temperature of the core-forming PtBS blocks). This complication can be avoided with PS-*b*-PA micelles, which have frozen PS cores with a high glass transition temperature (373 K).[14] Accordingly, at ambient temperatures, the size of the core and the aggregation number do not depend on the corona charge[5,11] and/or ionic strength (as will be shown in the present work). Information on the ionic distribution and spatial extension of the corona can hence be derived without complications related to changes in the aggregation number and/or the interactions among the hydrophobic units. As far as we are aware, such information is unavailable for simple ionic surfactant micelles, where the aggregation behavior actually depends on the charge and ionic strength of the supporting medium.[15] It is therefore of interest to investigate the contraction of the coronal layer and the concomitant effects on the chain statistics of the PS-*b*-PA micelles as a function of salt concentration and to explore to what extent the corona shrinks before the micelle eventually precipitates.

Detailed structural information about the morphology of the micelles is inferred from small-angle neutron scattering (SANS). The scattering is sensitive to the set of spatial Fourier transforms of the block density correlation functions, i.e., the partial structure factors.[16−18] The potential of the approach lies in its spatial resolution

together with the possibility to blank or highlight certain components in the complex mixture of copolymer blocks, solvent, and small ions. We will determine the individual partial structure factors pertaining to PS−PS and PA−PA density correlations, as well as the composition structure factor in the presence of various amounts of low molecular weight salt. The composition structure factor describes the correlation in the difference of the PS- and PA-block densities and is particularly sensitive to the ordering of the blocks within the micelle.

We will derive the aggregation number, core size, and physical extent of the corona from the scattering behavior. For this purpose, the structure factors are interpreted with radial density profiles pertaining to either a densely packed core or a corona with a certain chain statistics. It is shown that the core is invariant to the addition of salt. The corona chain statistics will be gauged from the scaling approaches including the balance of the conformational and osmotic stretching forces.[9,10] In the presence of salt, the difference in osmotic pressure of the co- and counterions inside and outside the micelle is obtained by employing the local electroneutrality condition and Donnan salt partitioning. With a sufficiently large fractional corona charge, a two-region model can describe the chain statistics. In the inner coronal region, where the local counterion concentration is much higher than the salt concentration, the density scaling is unaffected by the salt and is proportional to the inverse second power of the radial distance away from the core. For larger radial distances, screened electrostatic excluded volume effects govern the corona statistics with a density scaling similar to neutral star-branched polymers.[6] The contraction of the fully ionized micelle and the crossover distances between the two different scaling regimes are reported as a function of the salt concentration and interpreted with the scaling results for osmotic polyelectrolyte stars in the salt dominated regime. We will also investigate the effect of salt on the solubility and the structure of micelles with a low fractional corona charge 0.1, where the chain statistics is determined by charge annealing effects. The extent to which the micelle dimension and chain statistics can be controlled by the ionic strength, as opposed to the charge, will be explored.

Structure Factors

Contrast Variation. For a diblock $A(N_A)$-b-$B(N_B)$ copolymer solution, with N_A and N_B the number of monomers of block A and B, respectively, it is convenient to consider the blocks as the elementary scattering units.[19] Every block A is attached to a B block, and hence, the macroscopic block number densities exactly match the copolymer number density $\rho_A = \rho_B = \rho$. For an analysis of the scattering data, the copolymer solutions are considered a three-component system: two chemically different blocks immersed in a solvent. For such a three-component system, the coherent part of the solvent corrected SANS intensity reads

$$I(q)/\rho = \bar{b}_A{}^2 N_A{}^2 S_{AA}(q) + 2\bar{b}_A\bar{b}_B N_A N_B S_{AB}(q) + \bar{b}_B{}^2 N_B{}^2 S_{BB}(q) \quad (1)$$

with the block monomer scattering length contrasts $\bar{b}_A$ and $\bar{b}_B$, respectively.[20,21] In an H_2O/D_2O solvent mixture, the scattering length contrast is given by

(8) Misra, S.; Mattice, W. L.; Napper, D. H. *Macromolecules* **1994**, *27*, 7090.

(9) Borisov, O. V. *J. Phys. II* **1996**, *6*, 1.

(10) Borisov O. V.; Zhulina, E. B. *Eur. Phys. J. B* **1998**, *4*, 205.

(11) Groenewegen, W.; Lapp, A.; Egelhaaf, S. U.; van der Maarel, J. R. C. *Macromolecules* **2000**, *33*, 4080.

(12) Guenoun, P.; Davis, H. T.; Tirrell, M.; Mays J. W. *Macromolecules* **1996**, *29*, 3965.

(13) Guenoun, P.; Delsanti, M.; Gazeau, D.; Mays, J. W.; Cook, D. C.; Tirrell, M.; Auvray, L. *Eur. Phys. J. B* **1998**, *1*, 77.

(14) The actual value inside the core of aqueous copolymer micelles is unknown but is expected to be similar to the bulk value: Brandrup, J.; Immergut, E. H. *Polymer Handbook*, 3rd ed.; Wiley: New York, 1989.

(15) Sumaru, K.; Matsuoka, H.; Yamaoka, H.; Wignall, G. D. *Phys. Rev. E.* **1996**, *53*, 1744.

(16) Lovesey, S. W. *Theory of Neutron Scattering from Condensed Matter*; Oxford University Press: Oxford, U.K., 1984; Vol. 1.

(17) Higgins J. S.; Benoit, H. C. *Polymers and Neutron Scattering*; Oxford University Press: Oxford, U.K., 1994.

(18) Rawiso, M. *J. Phys. IV* **1999**, *9*, Pr1−147.

(19) Note that this definition differs from the situation for homopolymers, where the monomer is usually considered to be the elementary scattering unit.

$$\bar{b}_i = b_i - b_s \bar{v}_i / \bar{v}_s \quad b_s = X b_{D2O} + (1 - X) b_{H2O} \quad (2)$$

with X the D_2O mole fraction. The monomer $i = A$ and B and solvent s have scattering lengths b_i and b_s and partial molar volumes $\bar{v}_i$ and $\bar{v}_s$, respectively. The partial structure factors $S_{ij}(q)$ are the spatial Fourier transforms of the *block* density correlation functions

$$S_{ij}(q) = \frac{1}{\rho} \int_V d\vec{r} \exp(-i\vec{q}\cdot\vec{r})\langle \rho_i(0)\rho_j(\vec{r})\rangle \quad (3)$$

It is of particular interest to construct the composition structure factor

$$S_{AA}(q) - 2S_{AB}(q) + S_{BB}(q) =$$
$$\frac{1}{\rho} \int_V d\vec{r} \exp(-i\vec{q}\cdot\vec{r})\langle [\rho_A(0) - \rho_B(0)][\rho_A(\vec{r}) - \rho_B(\vec{r})]\rangle \quad (4)$$

This structure factor displays a maximum at wavelengths of the order of the inverse correlation distance between the A and B blocks. In the $q \to 0$ limit the composition structure factor goes to zero because macroscopic phase separation is impossible due to every A block is chemically connected to a B block. In the present experiments, the partial and composition structure factors are obtained by contrast variation in the water, i.e., by adjusting the solvent scattering lengths b_s through the D_2O mole fraction X.

Micelle Model. In a selective solvent, the copolymers form spherical aggregates with a hydrophobic A-block core and a coronal layer formed by the polyelectrolyte B blocks. For a monodisperse system and if the corona structure is invariant to fluctuations in intermicelle separation, the structure factor eq 3 takes the form

$$S_{ij}(q) = \frac{1}{N_{ag}} F_i(q) F_j(q) S_{cm}(q) \quad (5)$$

with the micelle aggregation number N_{ag}, the form factor amplitude $F_i(q)$, and the micelle center of mass structure factor $S_{cm}(q)$. In the absence of interactions between the micelles and/or at sufficiently high values of momentum transfer $S_{cm}(q)$ reduces to unity. The form factor amplitude $F_i(q)$ can be expressed in terms of the radial core ($i = A$) or corona ($i = B$) density $\rho_i(r)$

$$F_i(q) = \int_{V_{micelle}} d\vec{r} \exp(-i\vec{q}\cdot\vec{r})\rho_i(\vec{r}) =$$
$$\int dr \sin(qr)/(qr)4\pi r^2 \rho_i(r) \quad (6)$$

The scattering amplitudes are normalized to N_{ag} at $q = 0$. With eq 5, the composition structure factor eq 4 reads

$$S_{AA}(q) - 2S_{AB}(q) + S_{BB}(q) =$$
$$\frac{1}{N_{ag}}[F_A(q) - F_B(q)]^2 S_{cm}(q) \quad (7)$$

The factorization of the structure factors into the intramicelle form factor amplitudes $F_i(q)$ and the inter-micelle structure factor $S_{cm}(q)$ is important in recognizing certain relations between the different partial structure factors and the data analysis procedure. The center of

mass structure factor $S_{cm}(q)$ is positive definite, since it represents a scattered intensity (i.e., a squared amplitude). The intensities eq 1 can now be expressed in terms of *two* factors $u_i(q)$ ($i, j = A, B$):

$$I(q)/\rho = [\bar{b}_A N_A u_A(q) + \bar{b}_B N_B u_B(q)]^2$$
$$u_i(q) = [S_{cm}(q)/N_{ag}]^{1/2} F_i(q) \quad (8)$$

rather than *three* partial structure factors $S_{ij}(q)$. As has been shown in ref 5 and below, explicit use of eq 5 in the data analysis procedure according to eq 8 (and, hence, with a concomitant reduction in number of adjustable parameters) results in improved statistical accuracy in the derived structure factors.

Scattering Amplitudes. For a dense core, the radial A-block density is uniform for $0 \le r \le r_c$ and given by $\rho_A(r)4\pi r_c^3/3 = N_{ag}$ and zero for $r > r_c$, with r_c the core radius. The core form factor amplitude now takes the form

$$F_A(q) = N_{ag}3(\sin(qr_c) - qr_c\cos(qr_c))/(qr_c)^3 \quad (9)$$

Expressions for the scattering amplitude of Gaussian chains with constant density in the coronal layer (and the interference with the spherical core) are available in the literature.[22] However, due to the relatively small core size and the mutual segment repulsion induced by the charge, the density in the coronal layer is nonuniform and varies along with the radius away from the core. To describe the corona structure we will adopt an algebraic radial B-block density profile

$$\rho_B(r) = \rho_B(r_c)(r/r_c)^{-\alpha} \quad r_c \le r \le r_o \quad (10)$$

where corona chain statistics determines the value of α and $\rho_B(r_c)$ is the density at the core–corona interface. The latter interfacial density is related to the outer micelle radius r_o through the normalization requirement (i.e., by integration of the radial profile)

$$4\pi\rho_B(r_c)(r_o^{3-\alpha}r_c^\alpha - r_c^3)/(3 - \alpha) = N_{ag} \quad (11)$$

We will calculate the scattering amplitude eq 6 with algebraic profile eq 10 by numeric integration, although complex analytical expressions are available.[23]

The algebraic profile eq 10 accounts for the *average* corona density scaling and neglects *fluctuations*. The effect of fluctuations on the scattering behavior is important when the momentum transfer is of the order of the correlation distance within the corona. Furthermore, they contribute to the corona structure factor S_{BB} only; the cross term S_{AB} is unaffected due to the heterodyne interference between the amplitudes scattered by the homogeneous core and heterogeneous corona.[24,25]

Corona Chain Statistics

The value of the density scaling exponent α is determined by the chain statistics in the coronal layer. In the present contribution, the corona statistics will be gauged from the scaling approaches for star-branched polymers. These polymers can also serve as a model for spherical diblock copolymer micelles; the presence of the core does not invalidate the scaling results. The fact that the coronal region cannot extend right to the center of the micelle

(20) Des Cloiseaux, J.; Jannink, G. *Polymers in Solution, Their Modelling and Structure*; Oxford University Press: Oxford, U.K., 1990; Chapter 7.
(21) Here, q denotes the momentum transfer and is defined by the wavelength λ of the radiation and the angle θ between the incident and scattered beam according to $q = 4\pi/\lambda \sin(\theta/2)$.

(22) Pedersen J. S.; Gerstenberg, M. C. *Macromolecules* **1996**, *29*, 1363.
(23) Förster S.; Burger, C. *Macromolecules* **1998**, *31*, 879.
(24) Auvray, L. *C. R. Acad. Sci. Paris* **1986**, *302*, 859.
(25) Auvray L.; de Gennes, P. G. *Europhys. Lett.* **1986**, *2*, 647.

merely sets a certain minimum correlation length (i.e., blob size) at the core−corona interface. In the scaling approach the blob size ξ is determined by the condition that the chain remains unperturbed within the blob.[26,27] Each blob contains g monomers, each monomer with a step length a_B. The blob size ξ relates to the number of monomers g according to

$$\xi \sim a_B g^{\nu} \tag{12}$$

with ν related to the chain statistics inside the blob; e.g., $\nu = 1/2$ if the chain is Gaussian and $\nu = 3/5$ with chain excluded volume interactions. For a star-branched spherical micelle, both g and ξ may vary along the radius r away from the core. The radial B-block segment density scales as the number of monomers $N_{ag}g(r)$ in the shell of radius r and thickness $\xi(r)$

$$\rho_B(r) \sim N_{ag}g(r)/(r^2\xi(r)) \tag{13}$$

and the exponent α in eq 10 can be derived from eqs 12 and 13, together with a certain radial dependence of the blob size $\xi(r)$.

In the case of a neutral star-branched micelle, close packing of the blobs in the shell of radius r implies the radial dependence of the blob size $\xi(r) \sim N_{ag}^{-1/2}r$. In this Daoud−Cotton expanding blob model, the density scaling takes hence the form $\rho_B(r) \sim a_B^{-1/\nu}N_{ag}^{(3\nu-1)/(2\nu)}r^{(1-3\nu)/\nu}$ and $\alpha = 1$ or $4/3$ without ($\nu = 1/2$) or with ($\nu = 3/5$) chain excluded volume interactions, respectively.[6] Borisov and Zhulina have derived scaling expressions for the size and radial density distribution of star-branched polyelectrolytes with and without screening by added salt.[9,10] Furthermore, due to the recombination and dissociation balance of the weak polyacid block, migration of charges toward the outer coronal region (charge annealing effects) might be important. Here, we will summarize the scaling results for polyelectrolyte stars, as far as they are relevant for the interpretation of the present scattering data. For a derivation of the pertinent equations, the reader is referred to the seminal paper by Borisov and Zhulina.[10]

It is convenient to start the analysis of the corona statistics from micelles with a large fraction f_q of ionized groups and no added salt. In this situation, charge annealing effects are unimportant, most of the counterions are trapped in the coronal layer, and the concomitant osmotic pressure gives the main contribution to the corona stretching force. The radial scaling of ξ can be derived from the balance of the elastic, conformational, stretching force, and the osmotic pressure exerted by the counterions trapped inside the blob. Since the fraction of trapped counterions does not vary along the radius, the blob size ξ is constant and is given by[10]

$$\xi \sim a_B f_q^{-\nu} \tag{14}$$

The formation of radial strings of blobs of uniform size and, hence, uniform mass per unit length results in a outer coronal density scaling

$$\rho(r) \sim N_{ag}a_B^{-1}f_q^{\nu-1}r^{-2} \tag{15}$$

and hence $\alpha = 2$. Due to space restrictions, in the inner-coronal region the blobs are expected to increase in size (with α of the order of unity) with increasing distance

away from the core until the critical size given by eq 14 is reached. However, in previous work we found no evidence for an inner-corona expanding blob region, which is related to the minimum correlation length at the core−corona interface set by the grafting density.[5] Our fully ionized samples are in the osmotic regime, and, without added salt, the chains in the coronal layer are near 100% stretched with a density scaling proportional to the inverse second power of the radius away from the core ($\alpha = 2$).

An additional screening of Coulomb interaction becomes important when the concentration ρ_s of added salt exceeds the concentration of counterions ρ_i in the coronal layer. The corona stretching force is now proportional to the difference in osmotic pressure of co- and counterions inside and outside the micelle. This difference in osmotic pressure can be obtained by employing the local electroneutrality condition and Donnan salt partitioning between the micelle and the bulk of the solution. The micelle outer radius is obtained by balancing the total osmotic stretching force with the elastic force. In the salt dominated regime (i.e., if $\rho_s \gg \rho_i$), the overall radius of the micelle scales as[10]

$$r_o \sim (a_B^2 N_{ag}f_q^2 N_B^3)^{1/5}\rho_s^{-1/5} \tag{16}$$

An increase in salt concentration results, hence, in a gradual contraction of the micelle, because of additional screening of the Coulomb repulsion among the ionized polyelectrolyte block monomers (i.e., a decrease in electrostatic excluded volume interactions). The radial dependence of the blob size

$$\xi(r) \sim (a_B^2 N_{ag}f_q^2 \rho_s^{-1})^{-1/3}r^{2/3} \tag{17}$$

is obtained from the local balance of differential osmotic force and the local tension in the star arms.[10] As each arm exhibits locally Gaussian statistics ($\xi \sim a_B g^{1/2}$), the B-block density profile can be derived from eqs 13 and 17 and reads $\rho(r) \sim (N_{ag}^2 f_q^{-2}\rho_s a_B^{-8})^{1/3}r^{-4/3}$. The radial decay of the monomer density is described by the same exponent as in neutral star-branched polymers with short-range chain excluded volume interactions in a good solvent. Accordingly, in the salt dominated regime ($\rho_s \gg \rho_i$), the corona density scaling exponent takes the Daoud−Cotton expanding blob value $\alpha = 4/3$. However, in contrast to neutral stars, the elastic blobs in partially screened polyelectrolyte stars have a blob-size scaling exponent $2/3$ (eq 17) rather than unity and hence they are not closely packed.

For polyelectrolyte stars at intermediate ionic strengths, Borisov and Zhulina proposed a multiple-region-scaling model. At small distances from the core, where $\rho_i(r) > \rho_s$, the corona statistics is not affected by the added salt. Here, the chains are extended in the radial direction with uniform mass per unit length ($\alpha = 2$, in the most inner-coronal region α may be of the order of unity due to space restrictions). With increasing distance away from the core, the local counterion concentration decreases, and for $r > r_s$ the screening is governed by the salt. Hence, in the outer coronal region, where $\rho_s \gg \rho_i(r)$, the corona density scaling exponent takes the value $\alpha = 4/3$. The crossover distance

$$r_s \sim (a_B^{-1}N_{ag}f_q^{\nu})^{1/2}\rho_s^{-1/2} \tag{18}$$

is determined by the equality of the local counterion concentration $\rho_i(r) = f_q\rho(r)$ in the coronal layer of the osmotic star (with radial density eq 15) and the salt concentration ρ_s in the bulk. With the addition of simple salt, the fully ionized micelle contracts according to eq 16 with a concomitant decrease in the crossover distance r_s

---

(26) de Gennes, P. G. *Scaling Concepts in Polymer Physics*; Cornell University Press: Ithaca, NY, 1979.

(27) Grosberg A. Yu.; Khokhlov, A. R. *Statitical Physics of Macromolecules*; American Institute of Physics Press: New York, 1994.

between the inner- and outer-corona scaling regimes with density scaling exponents $\alpha = 2$ and 4/3, respectively. The salt progressively penetrates the micelles, and the radial decay of the monomer density scaling in the outer region is similar to the situation for neutral star-branched polymers. The blobs are not closely packed however and increase in size away from the crossover according to eq 17. The inner-corona region, characterized by a uniform expansion of the branches, remains unaffected until the salt concentration competes with the salinity generated by the counterions coming from the polyelectrolyte.

PA is a weak polyacid, and at low fraction of ionized monomers ($f_q \ll 1$) the effects of charge annealing are important. In the simplest approximation, the *local* charge fraction $f_q(r)$ is determined by the (presumably r-independent) ionization constant K and the mass action law $K = \rho(r)f_q(r)^2/(1 - f_q(r)) \approx \rho(r)f_q(r)^2$. Because of the dissociation and recombination balance, the charge fraction is now no longer constant and increases according to $f_q(r) \sim r^{2/(1+\nu)}$. A remarkable result of this charge annealing effect is that the local tension in the branches now increases with increasing distance away from the core. As the branches become more extended with increasing r, the blob size ξ *decreases* $\xi(r) \sim a_B r^{-2\nu/(1+\nu)}$ and the monomer density decays faster $\rho(r) \sim N_{ag} a_B^{-1} r^{-4/(1+\nu)}$.[10] The density scaling exponent α takes the value 8/3 or 5/2 without ($\nu = 1/2$) or with ($\nu = 3/5$) volume interactions, respectively. Although the addition of salt might shift the recombination−dissociation balance and, hence, influence the ionization constant K (by replacing hydronium ions by cations from the salt), the corona scaling behavior is not affected. Furthermore, in our experiments, the added salt concentration is in excess of the counterion concentration and the additional screening results in a contraction of the coronal layer according to eq 16.

Experimental Section

Chemicals and Solutions. PS-*b*-NaPA was purchased from Polymer Source Inc., Dorval, Canada. The number average degrees of polymerization of the PS and PA blocks are 20 and 85, respectively.[28] PS-*b*-NaPA was brought in the acid form by dissolving it in 0.1 M HCl and extensive dialysis against water (purified by a Millipore system with conductivity less than $1 \times 10^{-6}\ \Omega^{-1}\ \mathrm{cm}^{-1}$). The residual sodium content in PS-*b*-PAA was checked by atomic absorption spectroscopy and was less than 0.001. Solutions were prepared by dissolving freeze-dried PS-*b*-PAA in pure water and/or D_2O at 350 K under continuous stirring for 6 h. Furthermore, to break up clusters of micelles, the solutions were sonicated (Bransonic 5200) for 30 min at room temperature. The sonication power was relatively low (190 W) and, hence, without risk of damage or decomposition of the block copolymers. Copolymer concentrations were determined by potentiometric titration of the polyelectrolyte block and are given in mol of PA/dm³. The solutions were subsequently neutralized with alkali to a degree of neutralization DN. The degree of neutralization is the molar ratio of (added) alkali and polyacid monomer.

For neutron scattering four sets of samples were prepared. Three sets were made with fully ionized copolymers (degree of neutralization DN = 1) with polyelectrolyte block monomer concentration 0.093 mol of PA/dm³ in 0.05, 0.2, and 1 M KBr, respectively. The fourth set contained solutions in 0.05 M KBr with the same copolymer concentration but partially neutralized

---

(28) The degree of polymerization of the PS block was determined by the manufacturer with size exclusion chromatography. For the PA block, use of the quoted degree of polymerization ($N_{PA} = 120$, determined from the ratio of the aromatic to the aliphatic protons in the NMR spectrum of the poly(styrene-*b-tert*-butyl acrylate) precursor) gives incorrect normalization of the PA−PA structure factor and incorrect limiting low-q behavior of the composition structure factor. In ref 5, N_{PA} was optimized by satisfying the normalization constraints and takes the value 85 monomers/copolymer chain.
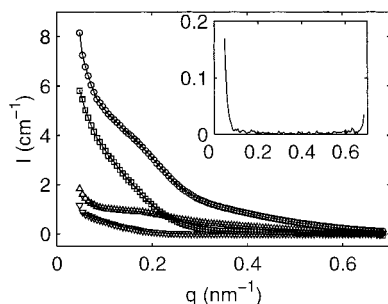
Table 1. Partial Molar Volumes and Scattering Lengths[a]

solute	$\bar{v}_i$ (cm³/mol)	$\bar{b}_i$ (10^{-12} cm)
PAA	48	$1.66 + 1.04X$
NaPA	34	2.40
KPA	40	2.40
PS	99	2.33
H_2O	18	−0.168
D_2O	18	1.915

[a] The PA partial molar volumes were taken from ref 33. X denotes the D_2O mol fraction (effect of exchangeable hydrogen). The polymer data refer to the monomeric unit.

Table 2. Scattering Length Contrast in 10^{-12} cm

solvent	$\bar{b}_{PS}$	$\bar{b}_{PAA}$	$\bar{b}_{NaPA}$	$\bar{b}_{KPA}$
H_2O	3.2	2.1	2.7	2.8
29% D_2O	0.0	0.8	1.6	1.4
50% D_2O (DN = 0.1)	−2.4	−0.1	0.7	0.5
70% D_2O (DN = 1)	−4.7	−1.0	0.0	−0.5
99% D_2O	−8.0	−2.3	−1.2	−1.8

to a degree 0.1. We have used KBr instead of NaCl to minimize an incoherent scattering contribution related to the salt. With added KBr concentrations greater or equal than 0.2 M, the partially neutralized (DN = 0.1) solutions are unstable and precipitate. For contrast variation, all solutions were prepared in H_2O and D_2O and subsequently mixed by weight to obtain four different H_2O/D_2O solvent compositions. The solvent compositions were checked by the values for transmission and with IR spectroscopy. Scattering length contrasts were calculated with eq 2 and the parameters in Table 1 and are collected in Table 2. Reference solvent samples with matching H_2O/D_2O composition were also prepared. Standard quartz sample containers with 0.1 cm (for samples in pure H_2O) or 0.2 cm path length were used.

Scattering. SANS experiments were done with the D22 diffractometer, situated on the cold source of the high neutron flux reactor at the Institute Max von Laue−Paul Langevin (ILL), Grenoble, France. The temperature was kept at 293 K. Samples were measured with two different instrument configurations. A wavelength of 0.8 nm was selected and the effective distances between the sample and the planar square multidetector (S−D distance) were 1.4 and 8.0 m, respectively. This allows for a momentum transfer range of 0.05−3.6 nm⁻¹. The instrument resolution is given by a 10% wavelength spread and an uncertainty in angle $\Delta\theta = 2.1 \times 10^{-3}$ and 3.4×10^{-3} for the 8.0 and 1.4 m S−D distance, respectively. The uncertainty in angle comprises contributions from the collimation, sample aperture, and detector cell size. The counting times were approximately 1 h/sample. Data correction allowed for sample transmission and detector efficiency. The efficiency of the detector was taken into account with the scattering of H_2O. Absolute intensities were obtained by reference to the attenuated direct beam, and the scattering of the pure solvent with the same H_2O/D_2O composition was subtracted. Finally, the intensities were corrected for a small solute incoherent contribution.

Neutron Data Analysis

For salt-free solutions, all ions come from the polyelectrolyte block, and there are four molecular components: solvent, the PS and PA blocks and counterions. The solvent is treated as a uniform background, and a description of the structure thus requires six partial structure factors. In previous work, we have shown that the structure factors pertaining to the counterions are very close to those involving the PA blocks.[11] Furthermore, it was shown that, within a 10% error margin, all counterions are trapped in the coronal layer. Accordingly, the PA-block scattering length contrast has been calculated by taking the relevant average of the contrast parameters of the PA in its acid and ionized forms including counterions (see Table 2). In addition, it is assumed that the ions from the added salt do not contribute to the scattering to any significant degree, because of negligible scattering length contrast. For an

Figure 1. SANS intensity versus momentum transfer from 0.1 mol of PA/dm^3 PS-*b*-PA solutions with DN = 1 in 1 M KBr. The H$_2$O/D$_2$O composition is 99, 0, 29, and 70% D$_2$O from top to bottom. The lines represent a two-parameter fit in which the partial structure factors are optimized. The inset displays the standard deviation of the two-parameter fit.
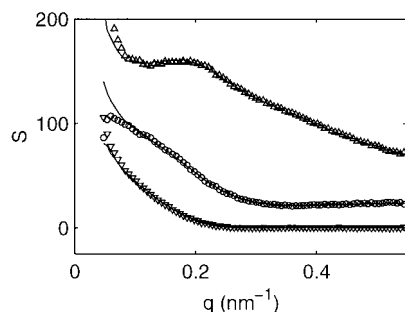

Figure 2. PS−PS (△), PS−PA (○), and PA−PA (▽) partial structure factors in 0.1 mol of PA/dm^3 PS-*b*-PA solutions with DN = 1 in 1 M KBr obtained from a three-parameter fit. The solid curves result from a two-parameter fit. To avoid overlap, the PS−PA and the PS−PS partial structure factors are shifted upward by 25 and 50 units, respectively.

analysis of the scattering data, the PS-*b*-PA/KBr solutions can, hence, be considered a three-component system and the structure is given by three partial structure factors describing the density correlations among the PS (=*A*) and PA (=*B*) blocks.

The PS−PS, PA−PS, and PA−PA partial structure factors are obtained from the scattered intensities of samples with contrast matching in the water. As an example, Figure 1 displays the intensities of fully ionized (DN = 1) 0.1 mol of PA/dm^3 PS-*b*-PA solutions in 1 M KBr. The data collected in the low *q* region is displayed only, where a strong change in intensity is observed with a variation in block contrast length parameters. Note that in 29% D$_2$O PS has negligible scattering length contrast and the intensity is directly proportional to the PA structure factor (Table 2). In 70% D$_2$O, the contributions to the scattering related to the PA blocks are approximately blanked. All samples show an upturn in intensity at very low values of momentum transfer $q < 0.07$ nm^{-1}. The low *q* upturn is due to clustering (secondary aggregation) of the micelles and is also observed in salt-free solutions.[5]

With four experimental intensities and three unknown partial structure factors, the data is overdetermined and the partial structure factors can be derived by orthogonal factorization in a least-squares sense (i.e., a three-parameter fit to four data points for every *q* value). The structure factors obtained from the intensities in Figure 1 are shown by the symbols in Figure 2. Note that the decomposition of the experimental intensities into the partial structure factors according to eq 1 is model-free; i.e., no assumptions regarding the morphology of the association structures have been made. In previous transmission electron microscopy and SANS work, it was

shown that the micelles are spherical and rather monodisperse in size.[5] The statistical accuracy of the derived partial structure factors can be improved if the spherical shape of the micelles is recognized.

For monodisperse spherical micelles, the partial structure factors can be expressed as a product of terms involving the radial core and/or corona profiles and a term describing the micelle center of mass structure factor (eq 5). As shown by eq 8, the intensities can now be expressed in terms of two unknown factors $u_i(q)$ rather than three partial structure factors $S_{ij}(q)$ (i, j = PS, PA). With a nonlinear least-squares procedure, the two factors $u_i(q)$ were fitted to the data and the partial structure factors were reconstructed according to $S_{ij}(q) = u_i(q)u_j(q)$. The fitted intensities and the derived partial structure factors are given by the solid curves in Figures 1 and 2, respectively. The statistical accuracy in the structure factors has now improved. In the low *q* (upturn) region, the standard deviation of the fit (inset of Figure 1) increases and the intensities do not comply with solvent composition independent structure factors. This shows that the samples differ in secondary aggregation, despite that they have been prepared in the same way (but in various H$_2$O/D$_2$O solvent ratios). For higher *q* values, the standard deviation levels off and the general behavior of the partial structure factors agrees with the results obtained from the model-free three-parameter fit. Accordingly, it is assumed that for *q* exceeding, e.g., 0.07 nm^{-1}, any clustering of the micelles does not influence the data.

All of the data was analyzed with the two-parameter procedure, and similar agreement was observed (intensities not shown). For the fully ionized samples with added KBr, the PS−PS (core) and PA−PA (corona) partial structure factors are shown in Figures 3 and 4, respectively. The PS−PA cross partial structure factor is not displayed. Instead, the composition structure factor eq 4 is more informative and is displayed in Figure 5. Figures 6 and 7 display the PA−PA and the composition structure factors for samples with 10% ionization of the polyelectrolyte block. For the latter samples, the PS−PS (core) partial structure factors are not shown, but they are similar to those pertaining to the fully ionized micelles in Figure 3. We have also included in Figures 3−7 the relevant structure factors of simple salt-free solutions from previous work.[5]

Core Structure

For the fully ionized micelles in Figure 3, the PS−PS (core) partial structure factors are compared to the form factor of a uniformly dense sphere [i.e., according to eq 5 with the square of the relevant scattering amplitude eq 9 and $S_{cm}(q)$ set to unity]. The form factor was convoluted with a Gaussian resolution function with the wavelength spread and uncertainty in angle given in the Experimental Section.[29] In the low-*q* range, the data deviate from the form factor. Without added salt, a correlation peak at $q_{max} = 0.12$ nm^{-1} and oscillatory behavior at higher *q* values is observed. With increasing ionic strength, the correlation peak shifts to higher values of momentum transfer ($q_{max} = 0.14$, 0.17, and 0.19 nm^{-1} in 0.05, 0.2, and 1 M KBr, respectively) and its intensity decreases. Furthermore, a concurrent peak broadening, a disappearance of the oscillatory behavior, and an intensity increase in the longer wavelength (smaller *q*) region is observed. Similar behavior is observed for the partially neutralized samples with DN = 0.1 (results not shown). The position of the
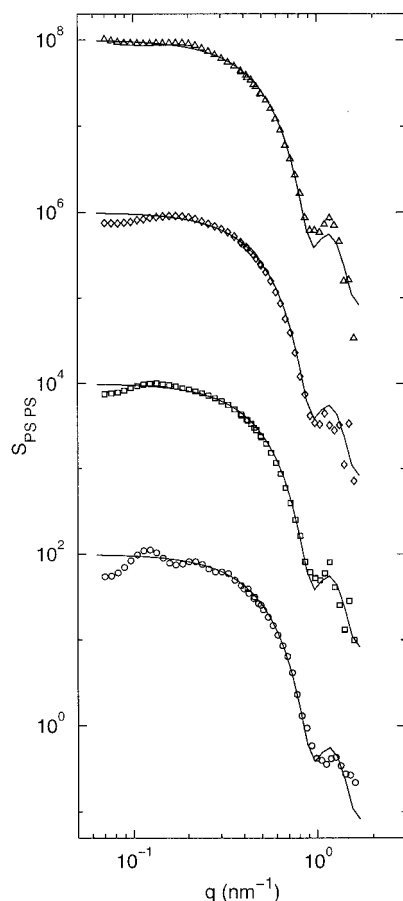
(29) Pedersen, J. S. *J. Phys. IV* **1993**, *3*, 491.

Figure 3. PS−PS partial structure factor versus momentum transfer for 0.1 mol of PA/dm³ PS-*b*-PA. The polyelectrolyte block is fully ionized (DN = 1). KBr concentrations: $\rho_s = 1$ M (△), 0.2 M (◇), 0.05 M (□), and salt-free (○) from top to bottom. The data are shifted along the *y*-axis with an incremental multiplication factor. The curves represent a fit with the form factor of a uniform sphere.

peak and the scaling with the micelle concentration (see ref 5), as well as the effects of the added salt, indicate that the origin of the peak is related to the ordering of the micelles. However, a complete discussion of the intermicelle solution structure is beyond the scope of the present contribution. Here, we will further focus on the intracore and intracorona structure, as can be gauged from the behavior of the structure factors at higher *q* values where intermicelle interference becomes progressively less important.

In the double logarithmic representation, the PS−PS partial structure factor displays an oscillation at $q \approx 1$ nm⁻¹. This feature corresponds with the (resolution broadened) first minimum and subsequent maximum in the sphere form factor and shows that the core is rather monodisperse in size. In the fit of the form factor, we have, hence, refrained from taking into account a polydispersity in core size. In the absence of intercore interference, the PS−PS structure factor is normalized to the aggregation number N_{ag} at $q = 0$. In the comparison of the sphere form factor with the data, N_{ag} and the core radius r_c were optimized and take the values 97 and 4.5 nm, respectively. As shown in previous work, N_{ag} and r_c comply with a densely packed and solvent excluded core formed by the PS blocks. Furthermore, it was shown that the core structure is not affected by the micelle concentration, the ionization of the corona-forming blocks, and/or the exchange of counterions.[5,11] The present results show that
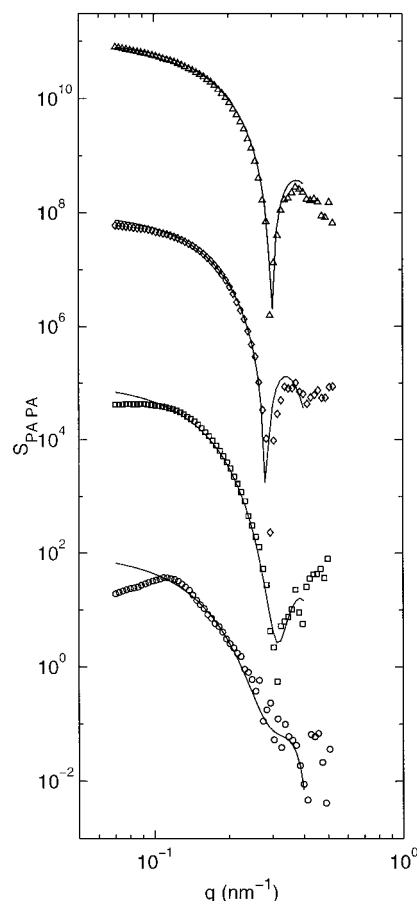

Figure 4. As in Figure 3, but for the PA−PA partial structure factor. The curves represent the PA form factor with an inner and outer corona density scaling exponent $a = 2$ and 4/3, respectively, together with the values for the crossover radial distances r_s listed in Table 3.

the addition of salt has also no effect on the self-assembling behavior. This is perhaps not a surprising result in view of the high glass transition temperature of the PS core (373 K). Accordingly, the core is in a glassy state and, once the micelles are formed, the core structure is invariant to factors related to concentration, charge, and screening of Coulomb interactions. We will further focus on the salt dependence of the micelle radius and corona statistics, which is reflected by the PA−PA (corona) and the composition structure factors.

Corona Structure

Full Corona Charge. First we will discuss the corona statistics of fully ionized micelles; the situation for the partially neutralized copolymers is different and will be detailed below. With increasing salt concentration, the corona shrinks and the structure factor scales toward higher values of momentum transfer with a concurrent sharpening of the minimum at $q \approx 0.3$ nm⁻¹ (see Figure 4). Furthermore, the correlation peak at finite wavelengths shifts to higher *q* values with an increase in intensity for longer wavelengths. This correlation peak is similar to the one observed in the core (PS−PS) structure factor and is due to the ordering of the micelles. In the case of star-branched polyelectrolytes with a relatively small number of arms (~12), a second peak at higher values of momentum transfer has been reported.[30] The latter peak is due

(30) Heinrich, M.; Rawiso, M.; Zilliox, J. G.; Lesieur, P.; Simon, J. P. *Eur. Phys. J. E*, in press.
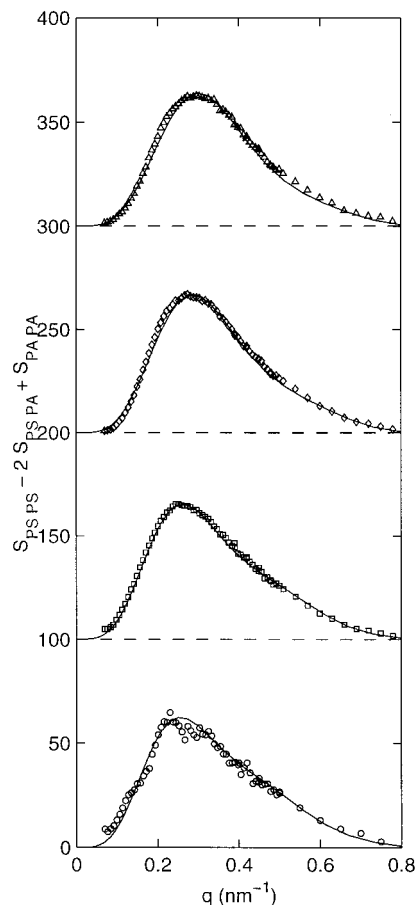
Figure 5. As in Figure 3, but for the PS−PS − 2PS−PA + PA−PA composition structure factor. The curves represent the intramicelle composition form factor with corona density scaling exponents as in Figure 4. The data are shifted upward along the y-axis with an increment of 100 units.
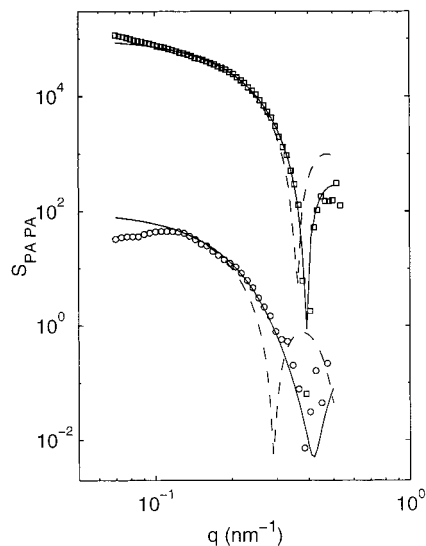

Figure 6. PA−PA partial structure factor versus momentum transfer for 0.1 mol of PA/dm³ PS-b-PA, but with 10% ionization of the polyelectrolyte block (DN = 0.1): 0.05 M KBr, □ (top) and salt-free, ○ (bottom). The data are shifted along the y-axis with a multiplication factor. The curves represent the PA form factor with corona density scaling exponent a = 8/3 (solid) and 4/3 (dashed).

to fluctuations and correlations among the branches within a single star. For the copolymer micelles, the corresponding intracorona correlation peak and the effect of corona chain
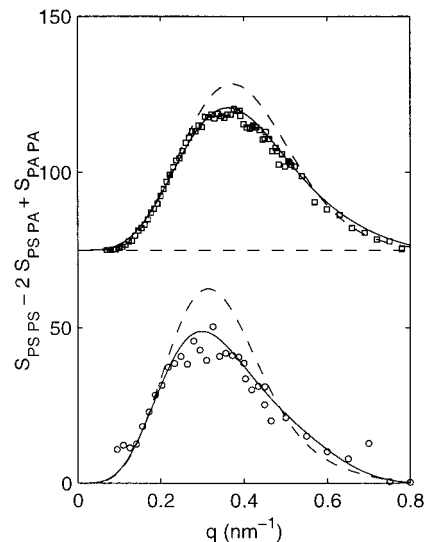

Figure 7. As in Figure 6, but for the PS−PS − 2PS−PA + PA−PA composition structure factor. The data are shifted upward with an increment of 75 units.

Table 3. Degree of Neutralization, DN, Salt Concentration ρ_s, Corona Density Scaling Exponent α, Core Radius r_c, Crossover Radius r_s, and Outer Micelle Radius r_o

DN	ρ_s (M)	α	r_c (nm)	r_s (nm)	r_o (nm)
1	0	2	4.5		24
1	0.05	2−4/3	4.5	13.5	22
1	0.2	2−4/3	4.5	8.0	19
1	1	2−4/3	4.5	5.5	17
0.1	0	8/3	4.5		20
0.1	0.05	8/3	4.5		15

fluctuations are beyond detection, because in the relevant q range (at $q \approx 0.7$ nm⁻¹)[5] the PA−PA structure factor is very small of the order of the experimental error margin. Furthermore, the micelle concentration is sufficiently low in the dilute regime such that the outer sections of the arms do not overlap. Accordingly, the PA−PA structure factors may be compared with the corona form factor calculated with an average density profile eq 10.

The corona form factor was calculated with eq 5 (with $S_{cm}(q)$ set to unity) and the scattering amplitude eq 6 with numeric integration of the algebraic density profile eq 10. Without added salt, the fully ionized PA chains in the coronal layer are near 100% stretched with a density scaling exponent $\alpha = 2$.[31] For the salt-free sample, the outer micelle radius r_o was optimized (with $\alpha = 2$), whereas the aggregation number and core radius were fixed at their values obtained from the normalization of the PS−PS structure factor (N_{ag} = 97, r_c = 4.5 nm, see ref 5). At full charge and minimal screening (no added salt), r_o takes the value 24 nm (Table 3).[32] Through the normalization requirement eq 11, the core and micelle radii as well as the aggregation number set the PA chain density at the core−corona interface $\rho_{PA}(r_c)$ (the grafting density is 1/2.6 nm⁻²). The latter interfacial density was subsequently fixed, and the data pertaining to samples with added salt were fitted with Borisov and Zhulina's two-region scaling model.[10] According to this model, the corona is divided

(31) A density scaling exponent α = 2 is also relevant for a radial string of blobs of uniform size.

(32) The fully stretched value of the radius amounts 25.5 nm, as estimated from the sum of the core radius 4.5 nm and the contour length of the PA block (85 monomers/chain with a vinylic step length 0.25 nm).

(33) Hiraoka, K.; Yokoyama, T. *J. Polym. Sci.: Polym. Phys.* **1986**, *24*, 769.

into two regions: an inner-coronal region where the chain statistics is not affected by the salt ($\alpha = 2$) and an outer region with a density scaling governed by screened electrostatic excluded volume interactions ($\alpha = 4/3$). The crossover distance r_s is the only adjustable parameter and determines, together with $\rho_{PA}(r_c)$, the outer radius r_o. The results are displayed in Figure 4, and the radii are collected in Table 3. In particular, the sharpening of the minimum at $q \approx 0.3$ nm^{-1} is nicely reproduced. With the addition of simple salt, the fully ionized micelle contracts with a concomitant decrease in r_s. Eventually, in 1 M excess salt, we almost recover the Daoud–Cotton expanding blob scaling model with $\alpha = 4/3$ (the optimized crossover distance between the two different scaling regimes becomes very close to the core radius). Further evidence for the salt-induced contraction is presented in the following, when the composition structure factor is discussed.

The composition structure factor eq 4 describes the spatial fluctuation of the difference in PS- and PA-block densities and is particularly sensitive to the intramicelle structure. The experimental results are displayed in Figure 5, together with the theoretical form factor expression eq 7 with $S_{cm}(q)$ set to unity. In the calculation of the composition form factor, the core, crossover, and outer radii [or $\rho_{PA}(r_c)$], as well as N_{ag}, were fixed at their values obtained from the PS–PS and PA–PA data (Table 3). With the two-region scaling model, the theoretical form factor expression predicts the block ordering satisfactorily. In particular, deviations from the single-micelle calculation are less prominent in comparison with the situation for the PS–PS and PA–PA structure factors. This is because the composition structure factor takes its maximum value beyond the intermicelle correlation peak. In the region of the correlation peak (at $q \approx 0.12$ nm^{-1}), the composition factor already approaches zero due to the chemical attachment of the PA and the PS blocks.

The composition structure factor shows a maximum at wavelengths of the order of the inverse correlation distance between the PA and PS blocks. The position of the maximum shifts toward higher q values with increasing salt concentration. This behavior is due to the contraction of the corona with increased screening of Coulomb interaction and is reproduced in the form factor with a variation of the crossover distance. The PA chains in the coronas of the micelles take an almost fully stretched configuration at high pH and no added simple salt. In excess salt (1 M KBr), the outer radius of the fully ionized micelles (17 nm, Table 3) approaches the value pertaining to the pure acid form at minimal screening conditions 15 nm.[5] Accordingly, despite the extremely high salt concentrations, the range in micelle dimension is similar to the one that can be covered by variation of the corona charge fraction (e.g., by variation of the pH of the supporting buffer medium).

The salt-induced contraction can be rationalized with the scaling results for star-branched polyelectrolytes.[9,10] For osmotic micelles in the salt dominated regime, the crossover and the micelle radii scale with the salt concentration according to $\rho_s^{-1/5}$ and $\rho_s^{-1/2}$ (eqs 16 and 18), respectively. The top and bottom panels of Figure 8 display the corresponding radii versus the relevant scaled inverse of the salt concentration. According to the scaling results there should be linear dependencies, which are indeed observed within the experimental accuracy. The crossover occurs at an optimized distance r_s, where the concentration of salt ions exceeds that of the corona segments by a factor 0.16, 0.22, and 0.52 in 0.05, 0.2, and 1 M KBr, respectively (note, however, that in 1 M the statistics is almost
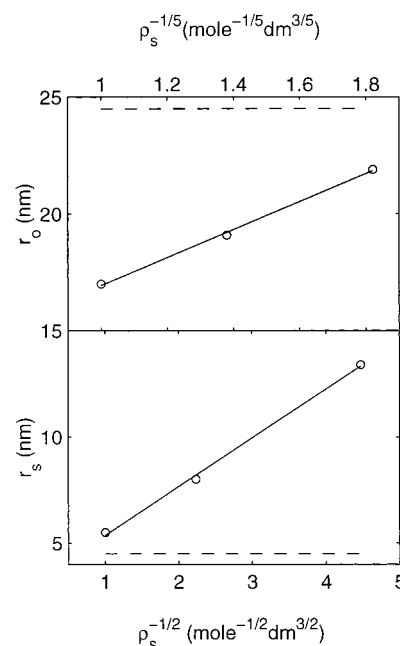

Figure 8. The outer micelle r_o (top) and crossover r_s (bottom) radii versus the scaled added salt concentration for fully ionized PS-*b*-PA (DN = 1). The top dashed curve represents the radius without added salt, whereas the bottom dashed curve denotes the core radius. The solid lines denote the respective scaling results for an osmotic polyelectrolyte star in the salt dominated regime.

completely governed by the salt). In view of the simplicity of the model (a gradual transition between the two different scaling regions is more likely to occur), this agreement between the counterion and salt concentrations at the crossover distance within half an order of magnitude can be considered quite gratifying.

Charge Annealing. In the case of low corona charge, one might expect to recover neutral polymer star behavior with a corona density scaling exponent of the order of unity. However, as shown in ref 5, for salt-free weak polyelectrolyte copolymer micelles at low degree of neutralization (DN $\lesssim$ 0.1) the scaling exponent has to be increased beyond the value 2 in order to get a satisfactory agreement between the data and the form factor expressions. Due to the dissociation and recombination balance of the weak polyacid, the charges preferentially migrate toward the outer-coronal region. As a consequence, the blob size decreases with increasing distance away from the core and the density scaling exponent takes the value 8/3 under θ-solvent conditions (5/2 including chain volume interactions). This peculiar behavior of the density scaling exponent based on charge annealing effects is reconfirmed by the present experiments on the partially ionized micelles in the presence of salt.

Figures 6 and 7 display the corona and the composition structure factors, respectively, of the 10% ionized micelles without added salt and in 0.05 M KBr. Note that at higher excess salt concentration, the quality of the solvent deteriorates and the micelles precipitate. Indeed, with $\alpha = 4/3$ poor agreement is observed between the form factors and the data, irrespective the presence of salt. A fit with the 2-4/3 two-region density-scaling model is also unsatisfactorily (results not shown). The minimum at $q \approx 0.4$ nm^{-1} in the PA–PA structure factor and the level of the maximum in the composition structure factors are nicely reproduced with $\alpha = 8/3$. With $\alpha = 5/2$ the agreement is somewhat worse (results not shown), but the experimental accuracy does not allow an assessment of the solvent

quality. The new results in excess salt reinforce our previous conclusion concerning the importance of charge-annealing effects at low fractional corona charge. In the calculation of the form factors, the outer radius r_o was optimized and the resulting values are also listed in Table 3. The interfacial density $\rho_{PA}(r_c)$ is now no longer constant but depends on the blob size at the core–corona interface (it is related to r_o through the normalization requirement eq 11). Again, with increasing salt concentration, a significant contraction of the micelles is observed, but the chain statistics seems not to be affected. Under excess salt conditions, just before the solubility threshold, the value of the radius of the 10% ionized micelle equals 15 nm (Table 3), which is exactly the same value as for the micelle in the salt-free pure acid form.[5]

Conclusions

We have obtained the individual partial structure factors pertaining to PS–PS and PA–PA density correlations, as well as the composition structure factor for samples with different amounts of added salt and/or fractional corona charge. The data were interpreted with a heterogeneous micelle model, i.e., a self-assembled spherical morphology consisting of a PS-block core, surrounded by a coronal layer formed by the PA-blocks. All the structure factors are sensitive to correlations among blocks pertaining to different micelles (intermicelle interference). In the composition structure factor, the latter effect is less prominent, because in the region of the correlation peak the composition structure factor already goes to zero due to the chemical attachment of the PA and the PS blocks. With increasing ionic strength, the correlation peak shifts to higher values of momentum transfer and its intensity decreases. Furthermore, a concurrent peak broadening, a disappearance of the oscillatory behavior, and an increase in intensity in the longer wavelength region are observed. However, the correlations among the micelles are beyond the scope of the present work and this part of the data still needs to be analyzed. Here, we have focused on the effect of supporting electrolyte on the intracore and intracorona structure.

From the PS–PS structure factor, it was observed that the addition of salt has no effect on the size of the core and the number of self-assembled copolymers per micelle. In previous works, it was already shown that the core structure is not affected by the micelle concentration, the fractional corona charge (i.e., pH), and/or the exchange of counterions.[5,11] This invariance to the various solution conditions is clearly due to the high glass transition temperature (373 K) of the core-forming PS blocks, whereas the experiments are done at room temperature. Changes in the size of the micelles are attributable only to the expansion/contraction of the ionic headgroup, i.e., the corona region of the micelle.

The PA–PA and the composition structure factor are sensitive to the salt-induced contraction and the density scaling of the corona. The fully ionized micelle is soluble at all added salt concentrations up to and including 1 M KBr. When every corona chain monomer carries a charge, a two-region density scaling model describes the corona involved structure factors satisfactorily. In the inner coronal region the density is proportional to the inverse second power of the radius away from the core; for larger radial distances the statistics are governed by screened

electrostatic excluded volume interactions with an $r^{-4/3}$ segment density scaling. The latter scaling is similar to the situation for neutral star-branched polymers including volume interactions. With increasing salt concentration, the micelle contracts with a concomitant decrease in the crossover distance between the two different scaling regimes. This behavior is manifested by, among others, a shift of the position of the maximum in the composition structure factor toward higher values of momentum transfer and a sharpening of the minimum at $q \approx 0.3$ nm^{-1} in the PA–PA (corona) structure factor, respectively. The crossover occurs at an optimized distance from the core, where the concentration of salt ions exceeds that of the counterions coming from the polyelectrolyte block by a factor ~0.2 (this value is the average in 0.05 and 0.2 M KBr; in 1 M the statistics is almost completely governed by the salt). The full range in chain statistics is covered: without salt the corona chains are almost fully stretched, whereas in 1 M salt the expanding blob model with $r^{-4/3}$ segment density scaling is almost recovered. In view of the simplicity of the model, the agreement between the counterion and salt concentrations at the crossover distance within half an order of magnitude is quite gratifying. Both the micelle and the crossover radii comply with the scaling results for osmotic polyelectrolyte stars in the salt dominated regime.

At 10% charge neutralization, we do not recover the $r^{-4/3}$ density scaling as observed for fully ionized micelles with high concentration of added salt. For low corona charge, the density scaling exponent has to be increased to a value 8/3 in order to reproduce the position of the minimum at $q \approx 0.4$ nm^{-1} in the PA–PA (corona) structure factor and the level of the maximum in the composition structure factor. A value of the scaling exponent larger than two reflects a *decrease* in blob size with *increasing* distance away from the core and can be rationalized in terms of a migration of the charges toward the outer region of the corona (due to the recombination and dissociation balance of the weak polyacid).[10] The present results reinforce our previous conclusion concerning the importance of these charge annealing effects at low degree of ionization ($\lesssim 0.1$).[5] For fractional charge 0.1, the addition of salt does not affect the corona density scaling to a significant degree, but the micelle nevertheless contracts and eventually becomes insoluble for $\rho_s \geq 0.2$ M.

In 1 M salt, the outer radius (17 nm) of the fully ionized micelle approaches the value pertaining to the pure acid form at minimal screening conditions (15 nm).[5] The latter value for the radius is also attained for 10%-ionized micelles in 0.05 M KBr, just before the solubility threshold. Accordingly, despite the extremely high salt concentrations required to compete with the salinity in the coronal layer generated by the counterions coming from the polyelectrolyte blocks, the range in micelle dimension is similar to the one that can be covered by variation of the fractional corona charge.